Report on the benchmarking of the event generator for specific reactions

1. Summary of the work performed

The goal of the Task 1 was to focus on the types of reactions for which test and improvements of the event generators were most urgently needed. Subtask 1 dealt with the extension of the intra-nuclear cascade and de-excitation models, already tested for proton-induced reactions between 200 and 2000 MeV, to light-ion induced reactions and down to the lowest possible energy (see D11.1). In Subtask 2, an event generator for heavy-ion induced reactions was developed (D11.2). More specific event generators solving particular deficiencies identified in the existing codes or important for a particular type of experiments were also investigated. They concern elastic proton-induced reactions (Subtask 3), delayed particle emission (Subtask 4), gamma rays from neutron-capture electromagnetic cascade (Subtask 5) and one-nucleon removal channel reactions (Subtask 8). Finally, a software tool was developed, which allows the use in GEANT4 of cross sections from correct (neutron and ions) reaction databases for low-energy reactions (Subtask 6).

This report summarizes very briefly the work already published or described in previous ENSAR reports. Only the work done in Subtask 8, which has just been finished, is detailed in section 6.

2. Subtask 3: Event generator for elastic proton-nucleus cross sections and p-n reactions with focus on exotic nuclei (UCM)

A procedure and codes to compute highly reliable elastic p-A and n-A cross-sections, in any kinematical situation (direct kinematics, inverse kinematics, other), in the range of energy from 20 to 1000 MeV/A and which can be applied to stable and exotic nuclei has been completed. It is based on the folding approach, and then the ingredients are proton and neutron densities, on one side, and NN effective interactions to cover the energy range on the other. A choice of sets from Hillhouse [4], Horowitz and Maxwell [3] and another set specifically developed for this project have been put together and tested for consistency.

For the other ingredient, the proton of nucleon densities, the codes offer several choices: numerical densities input by the user, empirical densities from J.D. Patterson, R.J.

Peterson Nuclear Physics A 717 (2003) 235-246, or HFB densities taken from http://www.astro.ulb.ac.be/bruslib/. A fourth case is an optimized density for ^{12}C to test the codes. These four choices cover an ample range of both stable and exotic nuclei, and the user just needs to input A and Z to the code. Extensive comparison of the results of this formalism to elastic proton and neutron scattering data from stable nuclei has been performed. The optical potentials which are derived have been also tested by comparing to inclusive neutrino-nucleus scattering [6]. The code includes necessary transformation and Jacobian needed for inverse (and other) kinematics. The user just needs to input the kinetic energy of both the lighter (p or n) and the heavier system. Angular cross-sections distributions, in the center of mass, lab system, inverse kinematics system and the user input kinematics are generated at the same time. Further, the tool has been also prepared to do inverse analysis, that is, to derive nuclear densities from the fit to elastic observables, especially for exotic nuclei where densities may not be well known and the user wants to derive them from measurements. A genetic algorithm developed in our group [7] has been applied for the densities fit to data. Figure 1 shows typical results for the elastic scattering of protons from different nuclei at various energies.

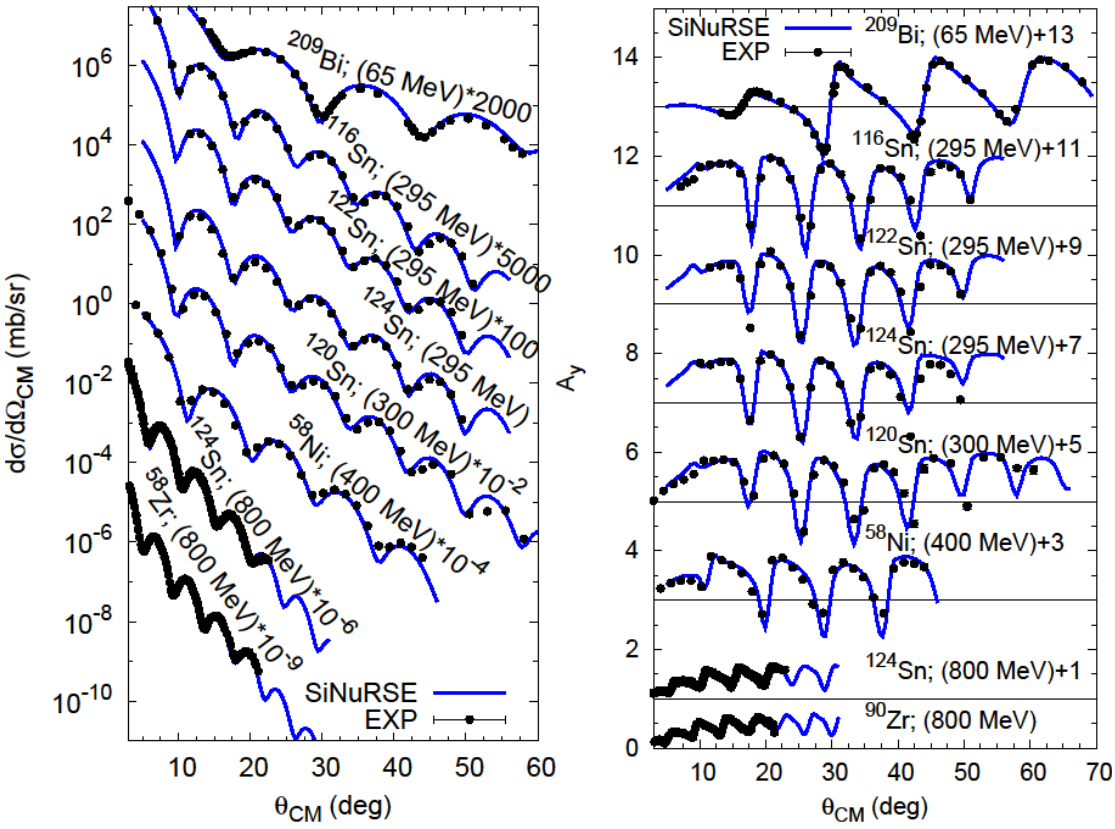

Figure 1. Differential cross sections and analyzing powers from the elastic scattering of 65 to 800 MeV protons from different nuclei using the formalism developed during the project.

3. Subtask 4: Development of an event generator for beta-decay including delayed particle emission (n, p, alpha) (IFIC)

The goal of the subtask was to develop a decay event generator which: 1) should be realistic in the sense of being capable to reproduce experimental results, 2) could be integrated in the Geant4 work frame, 3) be relatively simple to use by a non-expert user, and 4) which allows the more experienced user to modify the default parameters. In this sense, after considering different options, we decided to use consistently the information in the RIPL-3 Reference Parameter Library (R. Capote et al., Nuclear Data Sheets 110, p. 3107) as the default option. Known level schemes should be read directly from the corresponding tables prepared by T. Belgya. (http://www-nds.iaea.org/RIPL-3/levels/). Alternatively the interested user can process ENSDF databases and provide as input. Level densities will be obtained by interpolation from the tabulations prepared by Goliery, Hilaire et al. using HFB plus combinatorial calculations (http://www-nds.iaea.org/RIPL-3/densities/level-densities-hfb/). The tabulation also includes corrections whenever experimental data allows doing it. These level densities include parity asymmetries and enhancement effects due to collective phenomena in a natural way. Alternatively the interested user can provide level density parameters using the most common parameterizations (Back Shifted Fermi Gas, Constant Temperature, Gilbert-Cameron). For the gamma strength functions Lorentzian and Generalized Lorentzian shapes with parameters recommended by RIPL3 will be adopted. The interested user can override this parameterization. More difficult is to implement the case of delayed particle emission in a realistic way. This will call for the use of Optical Model calculated transmissions, which cannot be integrated in the event generator. In this case the default will be to use transmission coefficients for the square-well potential. However, we will give the option that the interested user calculates them externally (for example using Raynal's ECIS06 as included in TALYS-1.4 from Koning et al. http://www.talys.eu/) and pass them to the event generator. Code has been developed for some of the options and testing of the different algorithms could be done up to some point.

4. Subtask 5: Development of a gamma ray event generator for neutron capture electromagnetic cascades (CIEMAT).

The gamma-ray event generator for MF=6 evaluated data has been completed and included in the release of GEANT4.9.5. The description of the work has been published IAEA technical report INDC(NDS)-0612 (E. Mendoza et al.)

5. Subtask 6: Development of a software tool which allows the use in GEANT4 of cross sections from correct (neutron and ions) reaction data bases for low-energy reactions (CIEMAT)

The researchers of CIEMAT are members of the GEANT4 collaboration (Hadronic group) and included the software developments in the standard GEANT4 release (geant4.9.5 and later versions). Standard evaluated neutron cross-section libraries have been delivered to the IAEA nuclear data service (http://www-nds.iaea.org/geant4/) and are being maintained.

The distributed libraries have been validated for GEANT4 9.5 and an exhaustive comparison has been performed with the MCNPX code, running about 5000 simulations of identical geometries in both MCNPX and GEANT4 for all the isotopes in the recent ENDF-BVII.0, JENDL4.0 and JEFF.3.1.2 libraries. The comparison has allowed correcting major bugs in the neutron transport in GEANT4 9.5 and improving some of the secondary particle sampling models. Such changes have been included in GEANT4 9.6, which has been also thoroughly tested following the same procedure. Additional improvements are under investigation and will become available in future GEANT4 releases.

In addition, a similar package has been developed for the charged particle transport, using the TENDL libraries. A translation of the TENDL libraries into the GEANT4 format has been completed and the work will be included in future GEANT4 releases. It is expected that the package, called temporarily G4ParticleHP will combine G4NeutronHP with the new library driven particle transport. It is expected to have the code released together with GEANT4.10.

All the work described has been summarised in extensive reports.

6. Subtask 8: Improvement of Intra-Nuclear Cascade models for a better prediction of one-nucleon-removal channel (CEA)

Nuclear reactions between high-energy (>150 MeV) nucleons or hadrons and nuclei are usually described by means of intra-nuclear cascade (INC) models [8]. In this framework, the projectile is assumed to initiate an avalanche of binary collisions with

the nucleons of the target, which can lead to the emission of energetic particles. The nature of INC models is essentially classical. It is typically assumed that nucleons are perfectly localised in phase space and are bound by an average, constant potential; moreover, it is assumed that subsequent elementary collisions are independent.

It was realized some time ago that INC models systematically fail to describe inclusive cross sections for the removals of few nucleons [see e.g. 9, 10]. This is especially surprising in view of the fact that these observables are associated with peripheral reactions and mostly involve collisions between quasi-free nucleons; one would therefore expect intra-nuclear cascade to provide an accurate description of this particular dynamics. This puzzling result has been known for many years now, but no convincing explanation has ever been put forward.

We will show that the few-nucleon removal process at high energy is sensitive to the description of the nuclear surface, which we draw from a simple shell-model calculation. We will show that the predictions of an INC model [11] can be substantially improved by casting the shell-model calculation results in a form adaptable to the nuclear model underlying INC.

6.1. Model description

It is generally assumed that the first stage of high-energy nucleon-nucleus reactions can be described as an avalanche of independent binary collisions. The nuclear model underlying INC is essentially classical, with the addition of a few suitable ingredients that mimic intrinsically quantum-mechanical features of the initial condition and of the dynamics. At the end of the intra-nuclear cascade, an excited remnant is left. The de-excitation of this nucleus is typically described by a statistical de-excitation model.

In what follows, we shall make explicit reference to the Liège Intra-nuclear Cascade model, INCL [11] and the ABLA07 statistical de-excitation model [12]. The INCL/ABLA07 coupling is in general quite successful at describing a vast number of observables in nucleon-induced reactions at incident energies between ~ 60 and 3000 MeV [13]. The work described hereafter was performed with the latest C++ version of INCL, INCL++ [14].

The INCL model is peculiar in that it explicitly tracks the motion of all the nucleons in the system, which are assumed to move freely in a square potential well. The radius of the well is not the same for all nucleons, but it is rather a function R(p) of the absolute value of the particle momentum (which is a conserved quantity in absence of collisions). The initial particle momenta are uniformly distributed inside a sphere of radius p_F = 270 MeV/c. The relation between momentum and radius of the potential well is such that the space density distribution is given by a suitable Saxon-Woods parametrisation;

moreover, the nuclear surface is predominantly populated by nucleons whose energy is close to the Fermi energy [15].

6.2. One-nucleon-removal cross sections

Figure 2 shows the experimental data for one-nucleon removal in proton-induced reactions at energies between 500 and 1000 MeV, as a function of the target mass (all targets are β-stable). Calculations with INCL/ABLA07 are shown for comparison. It is clear that the model predictions are in the right ballpark for neutron removal, but they overestimate the proton-removal data by a factor that can be as large as 3-4 for heavy nuclei. Note also that other cascade models similarly overestimate the proton-removal cross sections. Figure 2 suggests that INC models might be affected by a fundamental defect. It is however rather surprising that the deficiency clearly manifests itself in proton removal, but neutron removal seems unaffected.

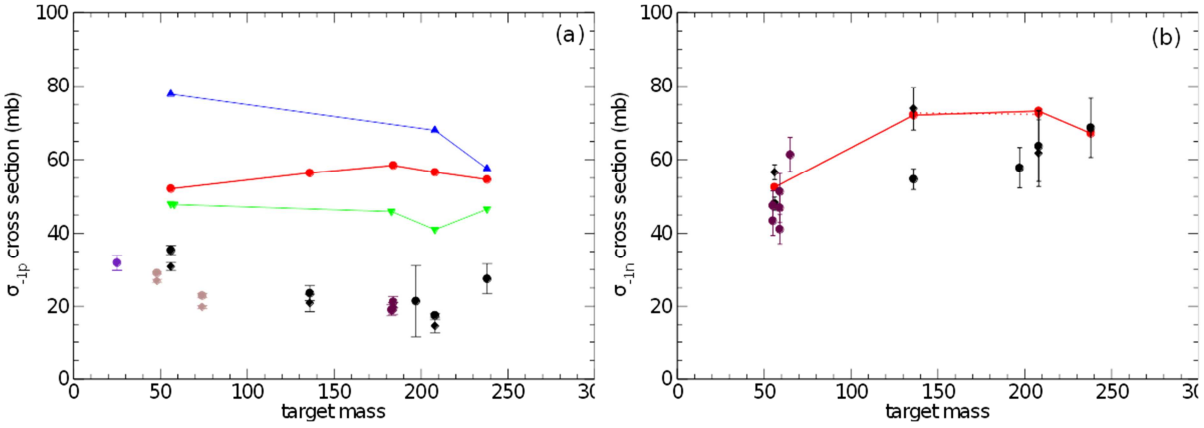

Figure 2: Experimental data for one-proton- (a) and one-neutron-removal cross sections (b) in proton-nucleus reactions above 500 MeV incident energy, as a function of the target mass. Diamonds refer to beam energies around 500 MeV, while circles represent energies between 800 and 1000 MeV. The solid curves represent calculations with INCL (red), Isabel (blue) [16] and Bertini [17] (green) at 1000 MeV. Experimental data are from Refs. [9, 18-27].

The analysis of the model calculations indicates that one-proton removal is dominated (about 90% of the cross section) by events with only one proton-proton collision. The two protons leave the nucleus, which however retains some excitation energy. If only one collision took place, the excitation energy is given by the energy of the proton hole, i.e. the difference between the Fermi energy and the energy of the proton that was ejected. This excitation energy is evacuated during the de-excitation stage by neutron evaporation. If the excitation energy is lower than the neutron separation energy, no particle will be evaporated and the energy will be evacuated as gamma rays; in this case the final (observed) residue will therefore be the target nucleus minus one proton. If the excitation energy allows for neutron evaporation, the final residue will be lighter (target

minus one proton minus x neutrons). The one-proton-removal cross sections are therefore extremely sensitive to the excitation energy left in the nucleus after the cascade. Note that there is a subtle difference between one-proton and one-neutron removal. One-neutron removal can be realized in two ways: either as a neutron ejection during INC followed by no evaporation (this is analogous to the proton-removal mechanism), or as no neutron ejection during INC followed by evaporation of one neutron.

Our results are essentially independent of the choice of the de-excitation model, since all of them employ very similar separation energies for stable nuclei. Comparison with the experimental data (Figure 2) seems to suggest that INC underestimates the excitation energy associated with the ejection of a proton; larger excitation energies would lead to increased neutron evaporation and would therefore reduce the one-proton-removal cross section.

6.3. Refinement of the INC nuclear model

We mentioned at the end of Section 6.2 that the nuclear surface is predominantly populated by nucleons whose energy is close to the Fermi energy. The ejection of one such nucleon during INC results in little excitation energy for the cascade remnant. However, even deeply-bound nucleons have a non-vanishing probability to be found in the nuclear surface; this aspect is usually neglected by INC models. Another detail that is usually neglected in the INC picture is the presence of neutron (or proton) skins in certain nuclei, such as ^{208}Pb. For surface reactions, this means that the local neutron density is several times larger than the proton density, leading to an enhanced probability for proton-neutron collisions.

	^{40}Ca - 1p	^{40}Ca - 1n	^{208}Pb - 1p	^{208}Pb - 1n
(a)	59.8	46.4	59.5	82.1
(b)	58.8	41.4	50.9	112.0
(c)	51.6	38.3	42.1	63.4
(d)	51.9	35.3	33.6	83.8
exp	54.7 ± 7.9	29.8 ± 6.4	17.6 ± 0.5	63.7 ± 9.6

Table 1: Cross sections for one-nucleon removal in 1-GeV p-nucleus reactions, with the following model variants: (a) standard, (b)standard plus skin, (c) standard plus surface fuzziness, (d) standard plus skin and surface fuzziness. Experimental data are taken from Refs. 23, 29. The experimental values for ^{40}Ca refer to an incident energy of 763 MeV.

6.4. Shell-model calculations

We have estimated the magnitude of both the effects above with a simple shell-model calculation. We assumed a central Saxon-Woods nuclear potential with a spin-orbit term

and a Coulomb term for the protons [28]. We numerically solved the radial part of the Schrödinger equation and determined the eigenfunctions and the eigenvalues of the bound states. The single-particle energies correctly reproduce the energies of the particle-hole states in ^{207,209}Pb and ^{207}Tl, ^{209}Bi.

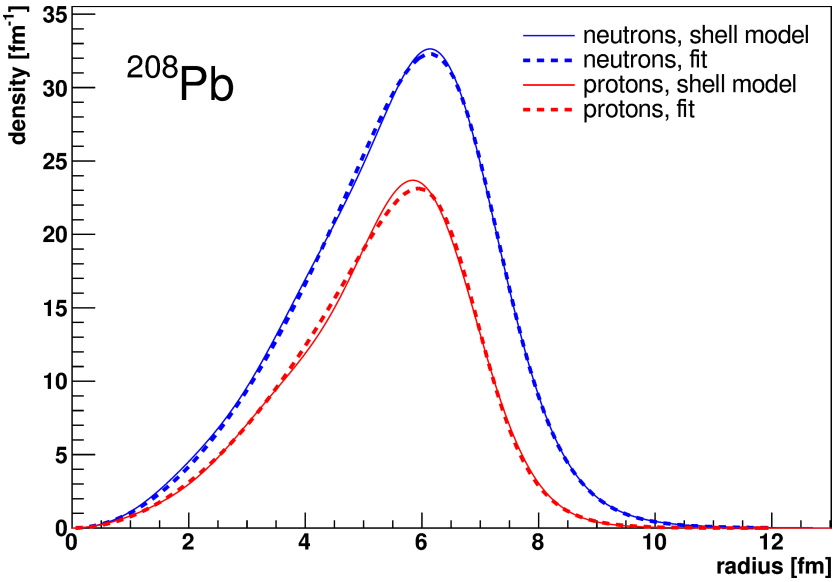

Figure 3: Proton (red) and neutron(blue) densities for ^{208}Pb. The thin solid lines represent the result of the shell-model calculation, while the thick dashed lines are Saxon-Woods fits.

We would like to use the shell-model proton and neutron densities as inputs for our INC calculation; however, the particle densities in INCL cannot be given by an arbitrary function, so we must somehow adapt the shell-model densities. We chose to fit them with Saxon-Woods distributions (shown in Figure 3 as dashed lines). The best-fit parameters show that the shell-model densities exhibit a neutron skin in ^{208}Pb. We have thus decoupled the INCL parameters describing the neutron space density from those describing the proton space density. The proton densities have not been modified (because they are already given by fits to the experimental charge radii), but the neutron parameters have been adjusted by the skin thicknesses resulting from the fit shown in Figure 3.

We have explained in the previous section that the outcome of single-collision cascades is sensitive to the energy of the ejected nucleon. We assume that the probability that a collision ejects a nucleon from a given shell is proportional to the local density of the shell orbital. Furthermore, we neglect rearrangement of the other nucleons in the Fermi

sea after the collision; this amounts to assuming that the excitation energy of the hole is simply given by the depth of the hole, measured from the Fermi energy.

With these assumptions, we can estimate the mean and RMS excitation energies that are left in the nucleus if a hole is punched in the Fermi sea at a certain distance from the center. These quantities are plotted in Figure 4 for the shell-model calculation and for the standard INCL nuclear model (f = 0).

It is clear from the results displayed in this picture that the standard INCL nuclear model yields mean and RMS excitation energies that are quite different from those resulting from the shell model. In the surface region, the proton mean and RMS values from INCL are sensibly lower than their shell-model counterparts, which seems to confirm that the excitation energy associated with the ejection of a proton is underestimated by INCL.

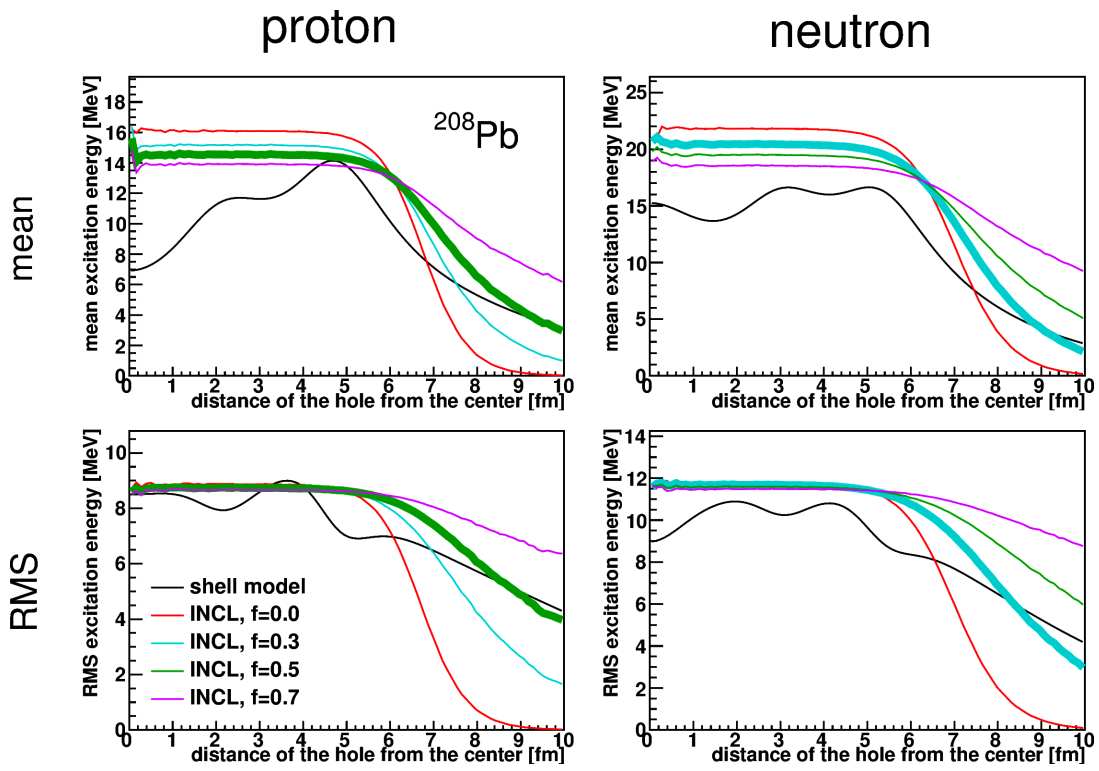

Figure 4 Mean (top) and root-mean-square (bottom) excitation energy induced by the presence of a proton (left) or neutron hole (right) in ^{208}Pb, as functions of the hole position. The black lines represent the shell-model result, while the colored lines are the results generated by the INCL nuclear model for different values of the fuzziness parameter f. The thick lines represent the selected parameter values.

6.5. Surface fuzziness

We mentioned in Section 2 that an INCL nucleon moves in a square-well potential whose radius R(p) depends on the nucleon momentum. The function R(p) is uniquely

determined by the choice of the space density ρ(r) and by the assumption that nucleon momenta are uniformly distributed in a sharp-surface Fermi sphere. We have shown above that this construction results in excitation energies for one-collision reactions that are much smaller than those resulting from the shell model and, arguably, than those suggested by the available experimental data.

We refine the INCL nuclear model by making R(p) into a random variable. We introduce a fuzziness parameter f ($0 \le f \le 1$) and a fuzzy square-well radius R(p,f). The precise definition of R(p,f) is outside the scope of this short paper, but it has the following properties: first, for f = 0 we recover the standard sharp correlation (R(p,0) = R(p)). Second, for given values of p and f , R(p,f) is a random variable that describes the radius of the square well. The fluctuations in R(p,f) are small if f is close to zero and they are large if f is close to one. Moreover, the fluctuations are constructed in such a way that the space density is still given by ρ(r) and the momentum density is still given by a sharp-surface Fermi sphere.

The construction of the refined INCL nucleus is analogous to the standard preparation algorithm [8]. The only difference is that the radius of the square-well potential is no longer in one-to-one correspondence with the nucleon momentum.

The refined nuclear model introduces fluctuations in the space distribution of nucleons with a given energy; equivalently, it introduces additional energy fluctuations for the nucleons found at a given position. Figure 4 indeed demonstrates that the average and RMS excitation energies for surface holes increase for increasing surface fuzziness, i.e. for increasing fluctuations. No value of the fuzziness parameter yields a good fit to the shell-model result, even if one limits oneself to the surface region. There is some degree of subjectivity in the choice of the best-fit values, which are taken to be f = 0.5 for protons and f = 0.3 for neutrons. For ^{40}Ca (not shown), the best-fit value was taken to be f = 0.3 for both protons and neutrons.

Summarizing, we have refined the INCL nuclear model in two respects. First, we have introduced a neutron skin, as described in Section 6.1. Second, we have introduced surface fuzziness, which increases the energy content of the nuclear surface and the probability for deep-nucleon removal in surface collisions. In the framework of the shell model, this effect is genuinely quantum-mechanical and is due to the penetration of the wave function in the classically forbidden region.

6.6. Results and conclusions

We turn now to the analysis of the results of the refined INC model. Table 1 shows how the neutron skin and the surface fuzziness affect the one-nucleon-removal cross sections in 1-GeV p+^{40}Ca and p+^{208}Pb. Unfortunately, no experimental data are available for

p+^{40}Ca at 1 GeV, but since we do not expect a strong dependence on the projectile energy, we can compare to Chen et al 's data at 763 MeV [29].

Several observations are due. First, the introduction of the neutron skin in ^{208}Pb boosts the neutron-removal cross section, as expected. This is however undesired, since the cross section calculated by standard INCL is already in moderate excess of the experimental value. Second, surface fuzziness suppresses the cross sections for both one-nucleon-removal channels. This is true both for ^{40}Ca and ^{208}Pb. Third, neither effect is sufficient to compensate for the overestimation of the proton-removal cross section in ^{208}Pb if considered alone.

When the two refinements are simultaneously applied to ^{208}Pb, the effect of surface fuzziness for neutron removal almost exactly compensates the effect of the neutron skin, and the final result (83.8 mb) is very close to the value calculated with standard INCL (82.1 mb), which is within two standard deviations (about 30%) of the experimental value. The proton-removal cross section, on the other hand, is reduced by almost a factor of two, which brings it much closer to the experimental datum, but not quite in agreement with it. The agreement for the p +^{40}Ca cross sections is also improved: the change in the proton-removal cross section is minor (~10%) and stays within the experimental error bar, but the neutron-removal cross section is reduced by ~50%, in fair agreement with the experimental value.

In conclusion, we have shown that INCL fails to describe the cross sections for one-nucleon removal at high energy. We have used simple shell-model calculations to show that the key to this deficiency lies in the presence of neutron skins in heavy, stable nuclei and in the energy content of the nuclear surface. In the future we will need to generalize our approach to non-magic nuclei and devise a systematic approach to the description of the properties of the nuclear surface.

This work has been submitted for publication [30].

7. References

[1] Murdock D P and Horowitz C J, Phys. Rev. C35, 1442 (1987)

[2] Horowitz C J and Serot B, Nucl. Phys. A368, 503 (1981)

[3] Maxwell O W, Nucl. Phys. A600, 509 (1996); A638, 747 (1998); A656, 231 (1999)

[4] Li Z P, Hillhouse G C, and Meng J; Phys. Rev. C77, 014001 (2008); C78, 014603 (2008)

[5] Clark B C, Mercer R L; Phys. Rev. C47, 297 (1993)

[6] Gonzalez-Jimenez R, Caballero J A, Meucci A, Giusti C, Barbaro M, Ivanov M V, Udias J M, Phys. Rev. C88, 025502 (2013)

[7] Fernández-Ramírez C, de Guerra EM, Udías A, Udías J M, Phys. Rev. C77, 065212 (2008)

[8] Serber R, Phys. Rev. 72, 1114 (1947)

[9] Jacob N P and Markowitz S S, Phys. Rev. C 11(2), 541 (1975)

[10] Audirac L, Obertelli A, Doornenbal P et al. Phys. Rev. C 88(4), 041602 (2013)

[11] Boudard A, Cugnon J, David J C, Leray S and Mancusi D, Phys. Rev. C 87, 014606 (2013) (Preprint 1210.3498)

[12] Kelić A, Ricciardi M V and Schmidt K H (2008) "ABLA07 – towards a complete description of the decay channels of a nuclear system from spontaneous fission to multifragmentation", Joint ICTP-IAEA Advanced Workshop on Model Codes for Spallation Reactions (Trieste, Italy: IAEA) p. 181 report INDC(NDC)-0530

[13] Leray S, David J C, Khandaker M, Mank G, Mengoni A, Otsuka N, Filges D, Gallmeier F, Konobeyev A and Michel R, J. Korean Phys. Soc. 59, 791 (2011); IAEA benchmark of spallation models (http://www-nds.iaea.org/spallations)

[14] Mancusi D, Boudard A, Cugnon J, David J C, Kaitaniemi P and Leray S, Phys. Rev. C 90(5), 054602 (2014)

[15] Boudard A, Cugnon J, Leray S and Volant C, Phys. Rev. C 66, 044615 (2002)

[16] Yariv Y and Fraenkel Z, Phys. Rev. C 20, 2227 (1979)

[17] Bertini H W, Phys. Rev. 131(4), 1801 (1963); Bertini H W, Phys. Rev. 188(4), 1711 (1969)

[18] Villagrasa-Canton C et al., Phys. Rev. C 75, 044603 (2007)

[19] Rejmund F, Mustapha B, Armbruster P et al., Nucl. Phys. A 683, 540 (2001)

[20] Giot L, Alcántara-Núñez J A, Benlliure J et al., Nucl. Phys. A 899, 116 (2013)

[21] Napolitani P, Schmidt K H, Tassan-Got L et al., Phys. Rev. C 76, 064609 (2007)

[22] Audouin L, Tassan-Got L, Armbruster P et al., Nucl. Phys. A 768, 1 (2006)

[23] Enqvist T, Wlazao W, Armbruster P et al., Nucl. Phys. A 686, 481 (2001)

[24] Taïeb J, Schmidt K H, Tassan-Got L et al., Nucl. Phys. A 724, 413 (2003)

[25]Titarenko Y E et al. (2002) "Experimental and theoretical study of the yields of residual product nuclei produced in thin targets irradiated by 100-2600 MeV protons", INDC report INDC(CCP)-434 IAEA, Nuclear Data Section, International Nuclear Data Committee (https://www-nds.iaea.org/publications/indc/indc-ccp-0434.pdf)

[26] Michel R, Gloris M, Lange H J et al., Nucl. Instrum. Meth. B 103, 183 (1995)

[27] Reeder P L, Phys. Rev. 178(4) 1795 (1969)

[28] Blomqvist J and Wahlborn S, Ark. Fys. 16 (1960)

[29] Chen C X, Albergo S, Caccia Z et al., Phys. Rev. C 56(3) 1536 (1997)

[30] Mancusi D, Boudard A, Carbonell J, Cugnon J, David J C, Kaitaniemi P and Leray S submitted to Phys. Rev. C.